J. Plasma Phys. (2025), *vol*. 91, E15
Published by Cambridge University Press

doi:10.1017/S0022377824001065

Measurement of the properties of the dust acoustic wave in a magnetic field

J.D. Williams [1],†, C. Royer[2], S. Chakraborty Thakur[2], E. Thomas Jr. [2] and S. Williams [2]

[1]Physics Department, Wittenberg University, Springfield, OH 45504, USA

[2]Physics Department, Auburn University, Auburn, AL 36849, USA

(Received 14 December 2023; revised 4 June 2024; accepted 5 June 2024)

We present the first experimental observations of the dust acoustic wave where the wave was observed to propagate in the directions of gravity and magnetic field when these directions were not aligned. The experiments were conducted in the Magnetized Dusty Plasma eXperiment facility using a novel electrode system that allows for the angle between gravity and the magnetic field to be varied in a controlled way. This letter reports on measurements in an rf glow discharge argon plasma environment where the angle between direction of gravity and the magnetic field is 45°. When there was no applied magnetic field, the wave was observed to propagate in the direction of gravity. However, as the magnetic field increased and the ions transitioned from flowing in the direction of gravity to the direction of the magnetic field, a second wave emerged and two distinct waves were observed to simultaneously propagate, one in the direction of gravity and one in the direction of the magnetic field. As the magnetic field was further increased, the wave that propagated in the direction of gravity was suppressed and the wave was only observed to propagate in the direction of the applied magnetic field. We also observe that the speed and the kinetic temperature of the dust for the mode that propagated in the direction of gravity decreased with increasing magnetic field while the speed and the kinetic temperature of the dust for the mode that propagated in the direction of the magnetic field increased with increasing magnetic field. These measurements suggest that an ion-dust streaming instability is at least partially responsible for the high temperatures that have previously been observed in dusty plasmas when the dust acoustic wave is present.

Keywords: complex plasmas, dusty plasmas

1. Introduction

Dusty plasmas are a four-component plasma systems composed of ions, electrons, neutral particles and charged microscopic particles, or ‘dust’. When the dust interacts with the other plasma species, it acquires a net charge and self-consistently modifies the properties of the surrounding plasma medium. The resulting system supports a range

† Email address for correspondence: jwilliams@wittenberg.edu

of new plasma phenomena (Morfill & Ivlev 2009; Melzer *et al.* 2021; Merlino 2021), including a collective mode known as the dust acoustic wave (DAW), a low-frequency, longitudinal wave that is self-excited by the free energy from the ion streaming through the dust component (Melandsø, Aslaksen & Havnes 1993; Rosenberg 1993; D'Angelo & Merlino 1996; Rosenberg 1996; Merlino 2009). Investigations of this wave mode have been a major topic of study for nearly 35 years (Merlino 2014). One observation from these investigations is that the dust kinetic temperature is observed to be quite large when this wave mode is present (Thomas, Fisher & Merlino 2007; Rosenberg, Thomas & Merlino 2008; Williams, Thomas & Marcus 2008; Fisher & Thomas 2010; Thomas 2010; Williams & Snipes 2010; Williams 2019). There have been a number of mechanisms proposed to explain these observations (Winske *et al.* 1995; Quinn & Goree 2000*a*,*b*; Joyce, Lampe & Ganguli 2002; Rosenberg 2002; Marmolino *et al.* 2009; Yaroshenko, Nosenko & Morfill 2010; Avinash, Merlino & Shukla 2011; Norman, Stegailov & Timofeev 2011; Fisher *et al.* 2013; Avinash 2015) but the physical mechanism responsible for the measured dust kinetic temperature remains an open question.

The presence of a magnetic field can substantially alter the properties of the plasma and this has led to a number of studies that have sought to understand how the DAW is affected by the presence of magnetic fields (Thomas *et al.* 2016; Tadsen, Greiner & Piel 2018; Choudhary *et al.* 2020; Melzer *et al.* 2020, 2021). In Tadsen *et al.* (2018) and Melzer *et al.* (2021), the magnetic field ($\leq$100 mT) and gravity were aligned and nanometre sized dust was used. As a result, gravity did not play a dominant role and the wave propagated radially outward from the central region of the dust cloud in the direction of the ion flow. In Thomas *et al.* (2016), Choudhary *et al.* (2020) and Melzer *et al.* (2020), the magnetic field ($\leq$ 150 mT–2 T) and gravity were aligned and micron sized particles were used. In these experiments, gravity played a dominant role and the waves were observed to propagate in the direction of gravity, the magnetic field and ion flow. In this Letter, we present the first measurements of the properties of the DAW with micron sized dust in the presence of a magnetic field when the magnetic field is not aligned with gravity. It is observed that, when there is no applied magnetic field, the wave is observed to propagate solely in the direction of gravity. However, as the magnetic field increased and the ions transitioned from flowing in the direction of gravity to the direction of the magnetic field, a second wave emerged and two distinct waves were observed to simultaneously propagate, one in the direction of gravity and one in the direction of the magnetic field. As the magnetic field was further increased, the wave that propagated in the direction of gravity was suppressed and the wave was only observed to propagate in the direction of the applied magnetic field.

2. Experiment

The experiments presented here were performed in the Magnetized Dusty Plasma eXperiment (MDPX), a high magnetic field research instrument capable of creating a uniform ($\leq$1 % variation) magnetic field up to 4 T over a 10 cm diameter $\times$6 cm long cylindrical region in the centre of the magnet (Thomas *et al.* 2015). A key feature of this instrument is the ability to rotate the magnet, allowing the angle between the direction of the magnetic field and gravity, α, to vary from 0 to 90°.

An argon plasma is generated at a neutral gas pressure of 66 mTorr by applying 1 W of rf power to an 11.5 cm diameter electrode. A second 11.5 cm diameter, electrically floating electrode is positioned 6.4 cm below the powered electrode. A copper ring (8.24 cm outer diameter, 6.34 cm inner diameter) is positioned on the lower electrode to increase confinement of the dust between the two electrodes, see figure 1(*a*). The electrode assembly is mounted to the vacuum chamber using a pair of ball bearings that allows electrode assembly to remain aligned with the direction of gravity as the magnet

https://doi.org/10.1017/S0022377824001065 Published online by Cambridge University Press

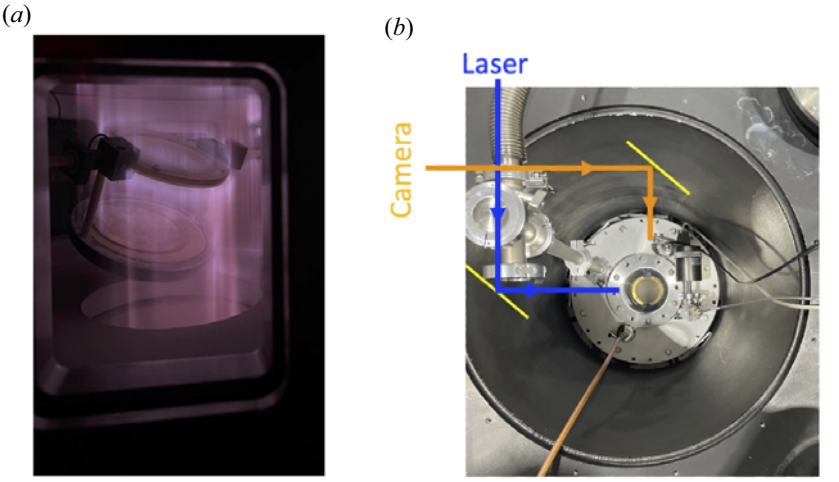

FIGURE 1. (*a*) Photograph of the electrode system with $\alpha = 22.5^{\circ}$. (*b*) Top view of the MDPX device showing the imaging system used. The yellow lines indicate a plane mirror.

and chamber are rotated. This allows, for the first time, the DAW to be examined in a configuration where the magnetic field is not aligned with the direction of gravity. Here, the angle between the direction of gravity and magnetic field is set to 45°.

Once the plasma is ignited, a dust dispenser is used to introduce 1 μm diameter silica ($\rho = 2000\,\mathrm{kg\,m^{-3}}$) dust into the plasma with magnetic field $B = 0\,\mathrm{T}$, and the plasma conditions are adjusted until the DAW is observed to propagate. For the experiments presented here, the wave mode is observed to fill the illuminated slice of the cloud. Further, based on the geometry of the electrode system, the ions stream away from the upper electrode in the direction of gravity and the wave is observed to initially propagate in the direction of the gravity when $B = 0\,\mathrm{T}$.

The dust is illuminated using a green, $\lambda = 532\,\mathrm{nm}$, laser that is expanded into a $\sim$3 mm thick, vertically aligned sheet. Image sequences were recorded at 200 frames per second using a USB3-based camera that has a linear light response and is positioned to view the system perpendicular to the laser sheet, see figure 1(*b*). The plasma parameters were measured in the central region of plasma where the dust clouds formed as a function of magnetic field using a Langmuir probe with no dust present and the dust density was found from the recorded images. It is noted that the voltage range used in the Langmuir probe measurements were carefully chosen to extract the relevant plasma parameters while avoiding the regime where the probe characteristics are severely distorted in the presence of the magnetic field, as previously reported in measurements in MDPX using a different electrode configuration (Williams *et al.* 2022). The experimental parameters are summarized in table 1.

Once the wave is observed, the strength of the applied magnetic field is increased. The effect of the magnetic field, $\boldsymbol{B}$, at pressure, p, is quantified using the ion Hall parameter, $H_{\mathrm{ion}} = \omega_{c,i}/\nu_{in} \sim B/p$, which is a ratio of the ion cyclotron frequency, $\omega_{c,i}$, to the ion neutral collision frequency, ν_{in}, and provides a measure of how magnetized the ions are. As the magnetic field increases and a threshold magnetic field is exceeded, $H \gtrsim 0.5$, a wave that propagates in the direction of the magnetic field emerges and it is observed that two distinct wave modes are observed to simultaneously propagate, see figure 2. Given that the DAW is excited by ions drifting through the dust (Melandsø *et al.* 1993; Rosenberg 1993;

https://doi.org/10.1017/S0022377824001065 Published online by Cambridge University Press

Parameter	Value
pressure, p (mTorr)	66
Electric field, E* (V m^{-1})	20–40
Magnetic field, B (T)	0.17–0.98
Electron temperature, T_e (eV)	2.75–4.3
Ion temperature, T_i* (eV)	∼0.025
Electron density, n_e (m^3)	0.87–2.5 × 10^{13}
Dust mass, m_d (kg)	1.05 × 10^{-15}
Dust density, n_d (m^3)	1.0–2.3 × 10^8
Ion hall parameter, H_{ion}**	0.5–1.5
Dust charge, Z_d^{**} (q_e)	1500–3000
Electron thermal:drift velocity, $\frac{u_{eo}}{v_{Te}}^{**}$	0.22
Ion thermal:drift velocity, $\frac{u_{io}}{v_{Ti}}^{**}$	1.54
Electron–neutral collision frequency, ν_{en}^{**} (Hz)	4.58–5.48 × 10^7
Ion–neutral collision frequency, ν_{in}^{**} (Hz)	2.70–2.71 × 10^5
Dust–neutral collision frequency, ν_{dn}^{**} (Hz)	79.48
Electron cyclotron frequency, ω_{ce}^{**} (Hz)	3.13–9.40 × 10^{10}
Ion cyclotron frequency, ω_{ci}^{**} (Hz)	0.43–1.29 × 10^6
Dust cyclotron frequency, ω_{cd}^{**} (Hz)	0.06–0.19

TABLE 1. Summary of measured, estimated* and calculated** parameters.

D'Angelo & Merlino 1996; Rosenberg 1996; Merlino 2009), the emergence of a second wave suggests that the direction of the ion flow through the dust cloud is changing. During this transition, as the ions become magnetized, there is a component of the ion flow that is in the direction of gravity and in the direction of the magnetic field. As the magnetic field continues to increase and the ions are fully magnetized, the ions flow is exclusively in the direction of the magnetic field and the component of the wave propagating in the direction of gravity is suppressed, $H \gtrsim 1.5$. At these higher magnetic field values, the wave is only observed to propagate in the direction of the magnetic field. As the magnetic field increases further, the wave propagating in the direction of the magnetic field is also suppressed, similar to previously observations (Tadsen *et al.* 2018; Choudhary *et al.* 2020; Melzer *et al.* 2020).

3. Results

To quantify the wave properties, a standard process is employed (Flanagan & Goree 2010; Menzel, Arp & Piel 2010; Killer & Melzer 2014; Williams 2014; Thomas *et al.* 2016; Williams 2019). After applying a Gaussian filter to the acquired images to remove the granularity of individual dust grains, the image intensity is measured along the direction of wave propagation (i.e. along a line that is perpendicular to the wave fronts) as a function of time. For the measurements reported here, the waves were observed to propagate in either the direction of gravity, the direction of the applied magnetic field or in both directions simultaneously depending on the strength of the magnetic field, as illustrated in the inset of figure 2. The wave structure is then found by subtracting the background dust density from the measured intensity profiles and compiled into the space–time diagram of figure 3(*a*), where the bright bands indicate the propagation of individual wave fronts through the dust

https://doi.org/10.1017/S0022377824001065 Published online by Cambridge University Press

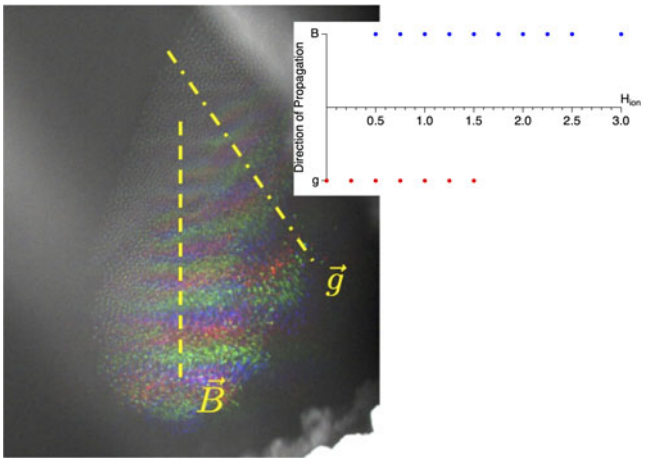

FIGURE 2. A superimposed image illustrating the propagation of the wave in the direction of gravity and the applied magnetic field, with each colour channel showing a snapshot of the wave at different times. Here, the red, green and blue channels show the wave at times t, $t + 15$ ms and $t + 30$ ms, respectively. The inset shows a plot depicting the observed direction of wave propagation as a function of ion Hall parameter, H_{ion}.

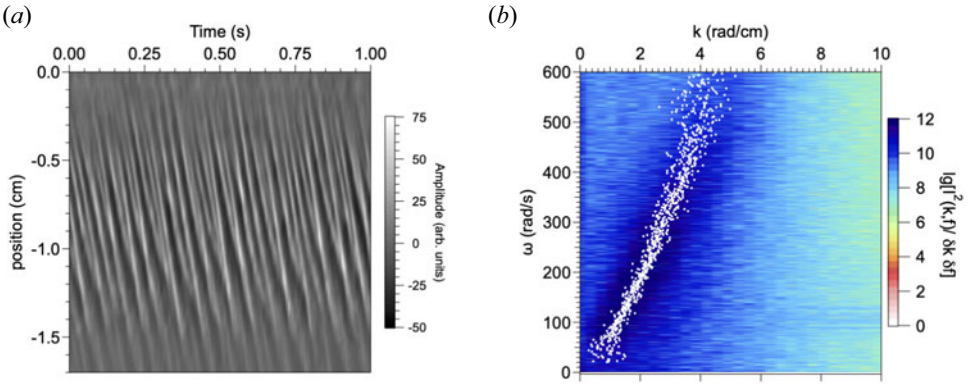

FIGURE 3. (*a*) Space–time plot showing the propagation of individual wave fronts through the dust cloud. (*b*) Representative dispersion relation for the component of the wave propagating in the direction of gravity with and ion Hall parameter of 0.5. Here, the white dots depict the extracted dispersion relation that was used in the subsequent analysis.

cloud. A two-dimensional Fourier transform is then performed and the peaks are extracted to determine the dispersion relation of the wave mode; see figure 3(*b*).

The phase velocity is found by tracking several wave fronts, which are observed to travel at a constant speed. The velocity of the wave is found by linearly fitting the location of the wave fronts as a function of time. The results of this analysis are seen in figure 4. It is observed that the phase velocity of the wave propagating in the direction of gravity is constant until the wave that propagates in the direction of the magnetic field emerges. At this point, the velocity of the wave propagating in the direction of gravity decreases as the magnetic field, H_{ion}, increases until this wave is suppressed at $H_{\text{ion}} > 1.5$. At the same time, the phase velocity of the wave that propagates in the direction of the magnetic field increases with increasing magnetic field strength. The phase velocity of the wave that

https://doi.org/10.1017/S0022377824001065 Published online by Cambridge University Press

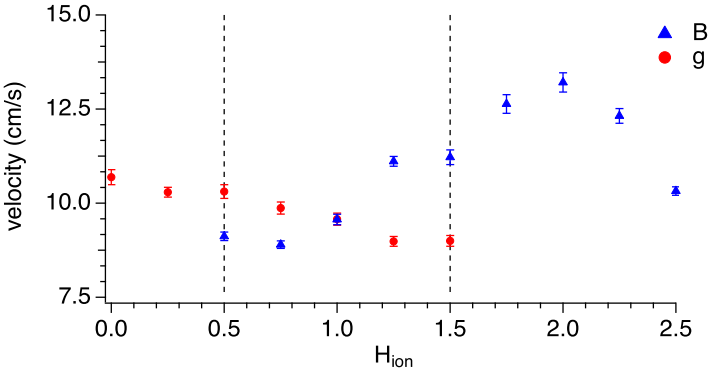

FIGURE 4. Plot of the wave speed as a function of the ion Hall parameter for the wave propagating in the direction of direction of (red circles) gravity and (blue triangles) magnetic field with $\alpha = 45^{\circ}$. The space between the vertical dashed lines indicates the range of ion Hall parameters where the wave mode was observed to simultaneously propagate in the directions of gravity and the magnetic field.

propagates in the direction of the applied magnetic field is observed to remain constant once the wave that propagated in the direction of gravity is suppressed. This behaviour follows from the motion of the ions, which change from travelling in the direction of gravity to the direction of the magnetic field as the ions become tied to the magnetic field with increasing field strength. With a smaller component of the ion motion in the direction of gravity, there is a decrease in the free energy from the ion streaming through the dust component that drives this component of the wave, resulting in the wave slowing and being suppressed. At the same time, there is an increasing component of the ion motion in the direction of the magnetic field with increasing magnetic field strength, resulting in an increase in the free energy in the direction of the magnetic field and the emergence of a wave that propagates in the direction of the magnetic field. This suggest that, once the wave that propagates in the direction of the gravity is suppressed, the ions only flow in the direction of the magnetic field and, at this point, a constant phase velocity is observed. Above a critical magnetic field strength, the phase velocity of the wave that propagates in the direction of the magnetic field decreases as the wave is suppressed. This suppression at higher magnetic fields has been previously observed (Tadsen *et al.* 2018; Choudhary *et al.* 2020; Melzer *et al.* 2020) but it remains unclear what mechanisms may be contributing to the observed wave suppression with increasing ion magnetization. This will need to be explored in future experiments through a combination of studies at higher magnetic fields and lower neutral pressures.

It is also observed that the dispersion relation of the modes of the DAW that are observed to propagate change as the magnetic field increases, see figure 5. It is observed that the dispersion relations for the two modes are the same at smaller values of the magnetic field, see figure 5(*a*). However, as the magnetic field increases, the dispersion relation of the wave that propagates in the direction of gravity and the magnetic field diverge, see figure 5(*b*). In particular, the slope for the mode propagating in the direction of gravity becomes more shallow while the dispersion relation for the mode propagating in the direction of the magnetic field becomes steeper. Based on previous measurements (Thomas *et al.* 2007; Rosenberg *et al.* 2008; Williams *et al.* 2008; Fisher & Thomas 2010; Thomas 2010; Williams & Snipes 2010; Williams 2019), this suggests a redistribution of energy from the direction of gravity to the direction of the magnetic field, consistent with the idea that the DAW is driven by the free energy from the ion streaming through the dust.

https://doi.org/10.1017/S0022377824001065 Published online by Cambridge University Press

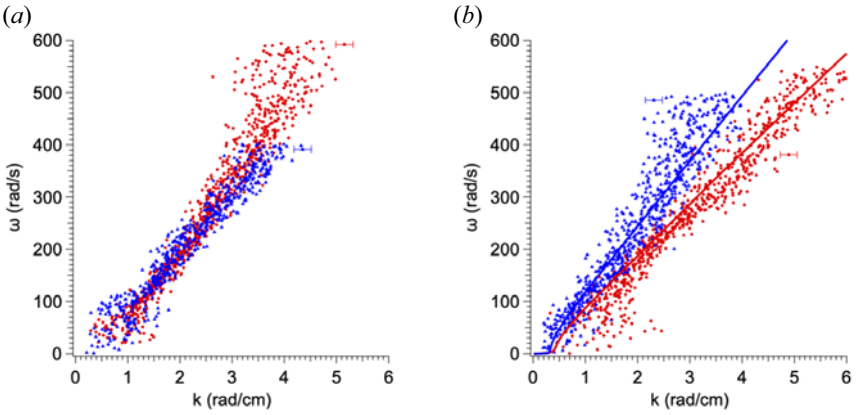

FIGURE 5. Plot of the dispersion relation for the wave propagating in the direction of (red) gravity and (blue) the magnetic field with $\alpha = 45^\circ$ when the ion Hall parameter is (*a*) 0.5 ($B =$ 0.178 T) and (*b*) 1.25 ($B = 0.446$ T). The dispersion relations in (*b*) are modelled using (3.1).

To quantify this, the dispersion relations are fit to a fluid model where the electron, ion and dust susceptibilities are modified by the angle θ between wave propagation and magnetic field. Following the process detailed in D'Angelo & Merlino (1996) and including the effects of flows and drag forces due to the high neutral pressure Williams *et al.* (2008), the dispersion relation can be written in the format used in Tadsen *et al.* (2018)

$$1 + \sum_{j=i,e,d} \frac{\omega_{pj}^2 \Omega_{1cj}^2}{k^2 v_{Tj}^2 \Omega_{1cj}^2 - \Omega_{1j}\Omega_{2j}\Omega_{2cj}^2} = 0, \tag{3.1}$$

where we use the abbreviated quantities $\Omega_{1j} = \omega - \boldsymbol{k}\cdot\boldsymbol{u}_{jo}$, $\Omega_{2j} = \omega - \boldsymbol{k}\cdot\boldsymbol{u}_{jo} + \mathrm{i}\nu_{jn}$, $\Omega_{1cj}^2 = \Omega_{2j}^2 - \omega_{cj}^2\cos^2(\theta)$, $\Omega_{2cj}^2 = \Omega_{2j}^2 - \omega_{cj}^2$, with $j =$ ion, electron and dust, $\omega_{pj} = q_j\sqrt{n_j/\epsilon_o m_j}$ are the plasma frequencies, $v_{Tj} = \sqrt{k_B T_j/m_j}$ are the thermal velocities, $u_{jo} = q_j E_o/m_j\nu_{jn}$ are the drift velocities, $\omega_{cj} = q_j B/m_j$ are the cyclotron frequencies, ν_{jn} are the collision frequencies with neutral particles, q_j are the charges, m_j are masses, n_j are densities and θ is the angle between $\boldsymbol{B}$ and $\boldsymbol{k}$. It is noted that, when $\boldsymbol{k}$ and $\boldsymbol{B}$ are aligned, the dispersion relation used here reduces to the dispersion relation used in Williams *et al.* (2008).

Using the parameters in table 1, the dispersion relations are fit with the dust kinetic temperature, T_d, being the only free parameter. Representative fits for the wave travelling in the direction of gravity ($\theta = 45^\circ$) and the magnetic field ($\theta = 0^\circ$) with $H_{\mathrm{ion}} = 1.25$ are seen in figure 5(*b*) and excellent agreement is observed.

From the fits of the dispersion relation, the dust kinetic temperature is found as a function of magnetic field and is plotted over the full range of H_{ion} measured, see figure 6. Similar to previous measurements, the dust kinetic temperature is significantly higher than the other plasma components (Thomas *et al.* 2007; Rosenberg *et al.* 2008; Williams *et al.* 2008; Fisher & Thomas 2010; Thomas 2010; Williams & Snipes 2010; Williams 2019). Further, the dust kinetic temperature behaves in a similar fashion to the phase velocity. When $H_{\mathrm{ion}} < 0.5$, the wave is observed to only propagate only in the direction of gravity, suggesting that the ion flow is primarily in the direction of gravity. In this regime, the dust kinetic temperature is relatively constant. As the ions begin to become magnetized, $0.75 < H_{\mathrm{ion}} < 1.5$, the wave is observed to propagate in both the direction of

https://doi.org/10.1017/S0022377824001065 Published online by Cambridge University Press

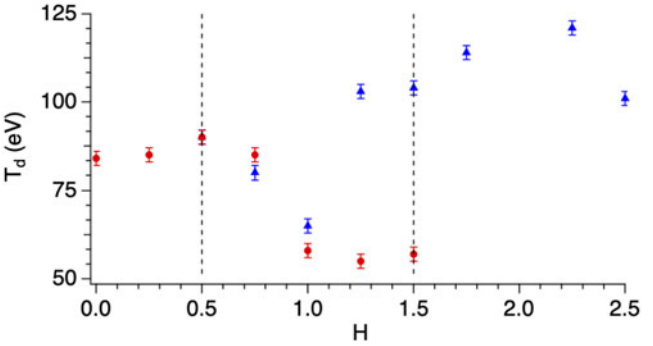

FIGURE 6. Plot of the dust temperature found by modelling the measured dispersion relations using (3.1) as a function of the ion Hall parameter for the wave propagating in the direction of (red circles) gravity and (blue triangles) the magnetic field with $\alpha = 45^\circ$. The space between the vertical dashed lines indicates the range of ion Hall parameters where the wave mode was observed to simultaneously propagate in the directions of gravity and the magnetic field.

gravity and magnetic field, suggesting that there is a component of the ion flow in each of these directions. As the magnetic field increases, the dust kinetic temperature is observed to be the same in both directions and to decrease, suggesting that the free energy from the ion streaming through the dust component is somewhat evenly split between the two modes of the wave observed. As the magnetic field continues to increase and there is a larger component of the ion flow in the direction of the magnetic field, there is a smaller component of the ion flow, and less free energy, in the direction of gravity, resulting in a decrease in the dust kinetic temperature for the wave propagating in the direction of gravity. At the same time, there is an increase in the temperature along the direction of the magnetic field due to the more free energy in the direction of the magnetic field. Once the ions are fully magnetized ($H_{\text{ion}} > 1.5$), the ions flow primarily in the direction of the magnetic field and the wave in the direction of gravity is suppressed. The dust kinetic temperature in direction of the magnetic field continues to increase slightly until the wave begins to be suppressed ($H_{\text{ion}} > 2.25$), at which point the dust kinetic temperature of the component of the wave in the direction of the magnetic field decreases. We note that, while a number of mechanisms have been proposed to explain the high dust kinetic temperatures (Winske *et al.* 1995; Quinn & Goree 2000*b*; Joyce *et al.* 2002; Rosenberg 2002; Yaroshenko, Verheest & Morfill 2007; Norman *et al.* 2011; Avinash 2015) observed, the exact mechanism is not known. The dependence of the dust kinetic temperature in the direction of gravity and magnetic field on the strength of the magnetic field observed here suggests that an ion-dust streaming instability (Winske *et al.* 1995; Joyce *et al.* 2002; Rosenberg 2002) is at least partially responsible for the high temperatures that have been observed.

4. Conclusion

In this Letter, we report on the first measurements of the DAW when the wave was observed to propagate in the direction of gravity and magnetic field when these directions were not aligned. As the magnetic field increased and the ions transitioned from flowing in the direction of gravity to the direction of the magnetic field, the wave propagating in the direction of gravity was suppressed and a wave propagating in the direction of the magnetic field emerged. It was observed that the speed and temperature of the dust for the wave that propagated in the direction of gravity decreased with increasing magnetic field

https://doi.org/10.1017/S0022377824001065 Published online by Cambridge University Press

while the speed and temperature of the dust for the wave that propagated in the direction of the magnetic field increased with increasing magnetic field. These measurements suggest that an ion-dust streaming instability may be at least partially responsible for the high temperatures that have previously been observed when the DAW is present.

Acknowledgements

The authors would like to thank J. Weaver, T. Weiss and G. Pahl (Wittenberg University) for their contributions to this work.

Editor Troy Carter thanks the referees for their advice in evaluating this article.

Funding

This work was supported by U.S. Department of Energy under grants DE-SC0021289, DE-SC0023820 (WU) and DE-SC-0019176 (AU), and the National Science Foundation under grant PHY-2010122 (WU) and NSF EPSCoR CPU2AL project via grant number OIA-1655280 (AU). The research activities of J.W. are also supported in part by the US National Science Foundation through its employee IR/D program.

Declaration of interests

The authors report no conflict of interest.

Data availability statement

The data that support the findings of this study are available from the corresponding author upon reasonable request.

REFERENCES

AVINASH, K. 2015 Theory of correlation effects in dusty plasmas. *Phys. Plasmas* **22** (3), 033701.

AVINASH, K., MERLINO, R.L. & SHUKLA, P.K. 2011 Anomalous dust temperature in dusty plasma experiments. *Phys. Lett.* A **375** (30-31), 2854–2857.

CHOUDHARY, M., BERGERT, R., MITIC, S. & THOMA, M.H. 2020 Influence of external magnetic field on dust acoustic waves in a capacitive RF discharge. *Contrib. Plasma Phys*. **60** (2), e201900115.

D'ANGELO, N. & MERLINO, R.L. 1996 Current-driven dust-acoustic instability in a collisional plasma. *Planet. Space Sci*. **44** (12), 1593–1598.

FISHER, R., AVINASH, K., THOMAS, E., MERLINO, R. & GUPTA, V. 2013 Thermal energy density of dust in dusty plasmas: experiment and theory. *Phys. Rev.* E **88** (3), 031101.

FISHER, R. & THOMAS, E. 2010 Thermal properties of a dusty plasma in the presence of driven dust acoustic waves. *IEEE Trans. Plasma Sci*. **38** (4), 833–837.

FLANAGAN, T.M. & GOREE, J. 2010 Observation of the spatial growth of self-excited dust-density waves. *Phys. Plasmas* **17** (12), 123702.

JOYCE, G., LAMPE, M. & GANGULI, G. 2002 Instability-triggered phase transition to a dusty-plasma condensate. *Phys. Rev. Lett*. **88** (9), 095006.

KILLER, C. & MELZER, A. 2014 Global coherence of dust density waves. *Phys. Plasmas* **21** (6), 063703.

MARMOLINO, C., DE ANGELIS, U., IVLEV, A.V. & MORFILL, G.E. 2009 On the role of stochastic heating in experiments with complex plasmas. *Phys. Plasmas* **16** (3), 033701.

MELANDSØ, F., ASLAKSEN, T. & HAVNES, O. 1993 A new damping effect for the dust-acoustic wave. *Planet. Space Sci*. **41** (4), 321–325.

MELZER, A., KRÜGER, H., MAIER, D. & SCHÜTT, S. 2021 Physics of magnetized dusty plasmas. *Rev. Mod. Plasma Phys*. **5** (1), 11.

MELZER, A., KRÜGER, H., SCHÜTT, S. & MULSOW, M. 2020 Dust-density waves in radio-frequency discharges under magnetic fields. *Phys. Plasmas* **27** (3), 033704.

MENZEL, K.O., ARP, O. & PIEL, A. 2010 Spatial frequency clustering in nonlinear dust-density waves. *Phys. Rev. Lett*. **104** (23), 235002.

MERLINO, R. 2021 Dusty plasmas: from Saturn's rings to semiconductor processing devices. *Adv. Phys.* X **6** (1), 1873859.

MERLINO, R.L. 2009 Dust-acoustic waves driven by an ion-dust streaming instability in laboratory discharge dusty plasma experiments. *Phys. Plasmas* **16** (12), 124501.

MERLINO, R.L. 2014 25 years of dust acoustic waves. *J. Plasma Phys*. **80** (6), 773–786.

MORFILL, G.E. & IVLEV, A.V. 2009 Complex plasmas: an interdisciplinary research field. *Rev. Mod. Phys*. **81** (4), 1353–1404.

NORMAN, G.E., STEGAILOV, V.V. & TIMOFEEV, A.V. 2011 Anomalous kinetic energy of a system of dust particles in a gas discharge plasma. *J. Expl Theor. Phys*. **113** (5), 887–900.

QUINN, R. & GOREE, J. 2000*a* Single-particle Langevin model of particle temperature in dusty plasmas. *Phys. Rev.* E **61** (3), 3033–3041.

QUINN, R.A. & GOREE, J. 2000*b* Experimental investigation of particle heating in a strongly coupled dusty plasma. *Phys. Plasmas* **7** (10), 3904–3911.

ROSENBERG, M. 1993 Ion- and dust-acoustic instabilities in dusty plasmas. *Planet. Space Sci*. **41** (3), 229–233.

ROSENBERG, M. 1996 Ion-dust streaming instability in processing plasmas. *J. Vac. Sci. Technol.* A **14** (2), 631–633.

ROSENBERG, M. 2002 A note on ion–dust streaming instability in a collisional dusty plasma. *J. Plasma Phys*. **67** (4), 235–242.

ROSENBERG, M., THOMAS, E. & MERLINO, R.L. 2008 A note on dust wave excitation in a plasma with warm dust: comparison with experiment. *Phys. Plasmas* **15** (7), 073701.

TADSEN, B., GREINER, F. & PIEL, A. 2018 Probing a dusty magnetized plasma with self-excited dust-density waves. *Phys. Rev.* E **97** (3), 033203.

THOMAS, E. 2010 Driven dust acoustic waves with thermal effects: comparison of experiment to fluid theory. *Phys. Plasmas* **17** (4), 043701.

THOMAS, E., FISHER, R. & MERLINO, R.L. 2007 Observations of dust acoustic waves driven at high frequencies: finite dust temperature effects and wave interference. *Phys. Plasmas* **14** (12), 123701.

THOMAS, E., KONOPKA, U., ARTIS, D., LYNCH, B., LEBLANC, S., ADAMS, S., MERLINO, R.L. & ROSENBERG, M. 2015 The magnetized dusty plasma experiment (MDPX). *J. Plasma Phys*. **81** (2), 345810206.

THOMAS, E., KONOPKA, U., MERLINO, R.L. & ROSENBERG, M. 2016 Initial measurements of two- and three-dimensional ordering, waves, and plasma filamentation in the magnetized dusty plasma experiment. *Phys. Plasmas* **23** (5), 055701.

WILLIAMS, J. 2019 Measurement of thermal effects in the dust acoustic wave. *IEEE Trans. Plasma Sci*. **47** (7), 3107–3112.

WILLIAMS, J.D. 2014 Time-resolved measurement of global synchronization in the dust acoustic wave. *Phys. Rev.* E **90** (4), 043103.

WILLIAMS, J.D. & SNIPES, E.K. 2010 Measurements of the dust temperature in the dispersion relation of the dust acoustic wave. *IEEE Trans. Plasma Sci*. **38** (4), 847–851.

WILLIAMS, J.D., THOMAS, E. & MARCUS, L. 2008 Observations of vertically propagating driven dust acoustic waves: finite temperature effects. *Phys. Plasmas* **15** (4), 043704.

WILLIAMS, S., CHAKRABORTY THAKUR, S., MENATI, M. & THOMAS, E. 2022 Experimental observations of multiple modes of filamentary structures in the magnetized dusty plasma experiment (MDPX) device. *Phys. Plasmas* **29** (1), 012110.

WINSKE, D., GARY, S.P., JONES, M.E., ROSENBERG, M., CHOW, V.W. & MENDIS, D.A. 1995 Ion heating in a dusty plasma due to the dust/ion acoustic instability. *Geophys. Res. Lett*. **22** (15), 2069–2072.

YAROSHENKO, V.V., NOSENKO, V. & MORFILL, G.E. 2010 Effect of strong electrostatic interactions of microparticles on the dust acoustic waves. *Phys. Plasmas* **17** (10), 103709.

YAROSHENKO, V.V., VERHEEST, F. & MORFILL, G.E. 2007 Dust-acoustic waves in collisional dusty plasmas of planetary rings. *Astron. Astrophys*. **461** (2), 385–391.